SCIENTIFIC REPORTS

OPEN

Notch-mediated inhibition of neurogenesis is required for zebrafish spinal cord morphogenesis

Received: 15 January 2019
Accepted: 18 June 2019
Published online: 10 July 2019

Priyanka Sharma, Vishnu Muraleedharan Saraswathy, Li Xiang & Maximilian Fürthauer

The morphogenesis of the nervous system requires coordinating the specification and differentiation of neural precursor cells, the establishment of neuroepithelial tissue architecture and the execution of specific cellular movements. How these aspects of neural development are linked is incompletely understood. Here we inactivate a major regulator of embryonic neurogenesis - the Delta/Notch pathway - and analyze the effect on zebrafish central nervous system morphogenesis. While some parts of the nervous system can establish neuroepithelial tissue architecture independently of Notch, Notch signaling is essential for spinal cord morphogenesis. In this tissue, Notch signaling is required to repress neuronal differentiation and allow thereby the emergence of neuroepithelial apico-basal polarity. Notch-mediated suppression of neurogenesis is also essential for the execution of specific morphogenetic movements of zebrafish spinal cord precursor cells. In the wild-type neural tube, cells divide at the organ midline to contribute one daughter cell to each organ half. Notch signaling deficient animals fail to display this behavior and therefore form a misproportioned spinal cord. Taken together, our findings show that Notch-mediated suppression of neurogenesis is required to allow the execution of morphogenetic programs that shape the zebrafish spinal cord.

The building of functional organs requires controlling the identity, shape and spatial arrangement of their constituent cells. Understanding how these aspects of embryogenesis are linked remains a major challenge. The Delta/Notch pathway governs the specification, proliferation, and differentiation of neuronal precursors in embryonic and adult tissues[1–5]. Notch receptors and Delta ligands are transmembrane proteins that elicit signaling between adjacent cells. In this context, the E3-Ubiquitin ligases Mindbomb and Neuralized promote an endocytic internalization of Delta ligand molecules that is required for Notch receptor activation[6–8]. Delta/Notch interactions then trigger a metalloprotease-mediated cleavage in the Notch extracellular domain, followed by a γ-Secretase-dependent intramembrane proteolysis that releases the Notch IntraCellular Domain (NICD) into the cytoplasm. NICD enters the nucleus to interact with CSL (for CBF1, Suppressor of Hairless, Lag1) family transcription factors and promote target gene transcription[1,4].

Several observations suggest that Notch signaling and neuroepithelial morphogenesis are functionally interdependent. Notch has notably been linked to the formation of radial glia[9–12], neural progenitor cells that present hallmarks of apico-basal polarity[13]. At the onset of neurogenesis, the neural plate of tetrapod embryos consists of a pseudostratified monolayer of apico-basally polarized cells which act as neural stem cells[13,14]. Following an expansion of this stem cell pool through symmetric divisions, some neural plate cells divide asymmetrically to generate the first neurons. Concomitant with this onset of neurogenesis, neural plate cells transform into radial glia[13]. During further development, radial glia cells undergo either symmetric, self-renewing divisions or divide asymmetrically to ultimately generate the majority of neurons that are present in the nervous system[13]. As radial glia cells retain most features of epithelial polarity, their presence is essential to maintain the epithelial architecture of the developing neural tube[10,13,15]. In addition to radial glia cells, studies in the mammalian and zebrafish Central Nervous System (CNS) have revealed the existence of Notch-responsive non-apical progenitor cells[13,16,17], identifying thereby an additional level of complexity in the relationships between the cellular organization of the neural primordium, Notch signaling and embryonic neurogenesis.

Université Côte d'Azur, CNRS, Inserm, iBV, Nice, France. Correspondence and requests for materials should be addressed to M.F. (email: furthauer@unice.fr)

In the forebrain of mice and zebrafish, cells undergoing neuronal differentiation present Delta ligands to neighboring progenitors to activate Notch signaling, induce radial glia identity, and thereby maintain neuroepithelial tissue organization[10,11]. Conversely, the apico-basal organization of the developing neural tube is itself required for Notch signaling as apical adherens junctions between nascent neurons and undifferentiating progenitors are required for Notch receptor activation[15,18].

In contrast to tetrapods, the initial stages of zebrafish spinal cord morphogenesis take place in a neural primordium that lacks a polarized epithelial architecture[19–23]. While the cellular organization of the zebrafish neural plate displays similarities to the pseudostratified epithelium of higher vertebrates[14,20,23,24], major hallmarks of apico-basal polarity such as apical Par protein localization, adherens junctions and tight junctions appear only after the beginning of neuronal differentiation, by mid-segmentation stages[19–23,25]. This raises the question whether and how Notch signaling and neuroepithelial morphogenesis are linked during zebrafish neural development?

A second particularity of the development of the zebrafish is the occurrence of a particular type of morphogenetic cell division[19,20,22,26]. In these so-called C-divisions, a cell originating from one side of the neural primordium divides at the embryonic midline so that one of its daughters integrates the contralateral half[19,22,26]. The apical polarity protein Partitioning defective 3 (Pard3) accumulates at the cytokinetic bridge which prefigures the future apical neural tube midline[22]. Neural primordia in which cell divisions have been blocked establish apico-basal polarity, but fail to form a straight, regular apical neural tube midline[27]. It has therefore been suggested that C-divisions, while not being absolutely required for the establishment of neural tube apico-basal polarity, confer a morphogenetic advantage to the embryo by relocating cells that would otherwise span the neural tube midline[20,23,27]. Despite the fact that C-divisions confer robustness to neural tube development, their regulation remains poorly understood. While Pard3 and Planar Cell Polarity (PCP) proteins are known to control C-divisions[22,26], the relationship between neurogenic Notch signaling and C-divisions has not been investigated.

In the present study, we inhibit Notch pathway activity and study the impact on zebrafish CNS morphogenesis. Our work reveals that the relationship between Notch signaling and neuroepithelial morphogenesis depends on the biological context. While some regions of the nervous system can acquire apico-basal polarity and neuroepithelial organization independently of Notch, Notch signaling is required for the morphogenesis of the dorso-medial spinal cord. In this tissue, Notch signaling is essential to inhibit neuronal differentiation and thereby allow the emergence of neuroepithelial identity and progressive epithelialization of the developing neural tube. Loss of Notch signaling also impairs the morphogenetic behavior of the cells of the neural primordium, thereby causing the formation of a misproportioned spinal cord. Our findings therefore show that beyond the control of the cellular composition of the nervous system, the ability of the Delta/Notch pathway to restrain neurogenesis is essential for the execution of morphogenetic programs that govern the shaping of the zebrafish spinal cord.

Results

Mindbomb1 is essential for zebrafish spinal cord morphogenesis. Genetic studies in zebrafish have identified the E3-ubiquitin ligase Mindbomb1 (Mib1) as a central regulator of Delta ligand internalization and Notch activation[6,28]. To study the role of Notch signaling in zebrafish CNS morphogenesis, we inactivated *mib1* using a validated Morpholino[29] and *mib1*^{ta52b} mutants[6]. In accordance with published observations[29], mib1 morphants presented an upregulation of DeltaD (DlD) due to a failure in Notch-dependent lateral inhibition, and a relocalization of DlD from endocytic compartments to the plasma membrane (Fig. 1a",b").

Antibody staining against the apical Par complex component atypical Protein Kinase C (aPKC[30]) was used to visualize apico-basal polarity. To analyze tissue morphology, fluorescent Phalloidin was used to visualize cortical F-actin. mib1 morphants display a loss of apical aPKC signal (Fig. 1b') and an overall disorganization of neuroepithelial tissue architecture in the anterior spinal cord (Fig. 1b). A similar loss of neuroepithelial polarity was observed in *mib1*^{ta52b} mutants (Fig. 1c,c'). Wild-type mib1 RNA injection rescued the polarity defects of *mib1*^{ta52b} mutants, warranting the specificity of our observations (Supplementary Fig. S1).

Our experiments show that loss of Mib1 impairs apico-basal polarity and epithelial organization in the zebrafish spinal cord. Accordingly, no polarized enrichment of the apical polarity proteins Pard3[31] (Fig. 1d,e), Crumbs[32] (Fig. 1f,g) and the tight junction component Zonula Occludens 1 (ZO-1[19], Fig. 1h,i) is detectable in *mib1*^{ta52b} mutants. In accordance with a failure to establish Par complex-dependent polarity, *mib1*^{ta52b} mutants fail to display the Pard3-dependent alignment of γ−Tubulin-positive centrosomes that is observed at the neural tube midline of wild-type siblings (Fig. 1j,k)[33].

The canonical Notch pathway is required for the morphogenesis of the zebrafish spinal cord. In addition to its role in Delta ligand internalization, Mib1 also regulates the ubiquitination and endocytic trafficking of other substrate proteins[34,35]. This raises the question whether the neuroepithelial defects of Mib1-depleted embryos are due to the loss of Notch signaling or to a Notch-independent function of Mib1? To address this issue, we interfered with different Notch pathway components and analyzed the effect on spinal cord morphogenesis.

Mib1 loss-of-function impairs the endocytosis of DlD, one of the two zebrafish homologues of mammalian Delta-like-1 (Dll1)[6,29]. Apico-basal polarity is however intact in *dld*^{ar33} mutants (Supplementary Fig. S2a,b). Mib1 also interacts with DeltaA (DlA), the second Dll1 homologue[36]. Accordingly, *mib1*^{ta52b} mutants display excessive cell surface accumulation of DlA (Fig. 2a,b). Injection of a validated dla morpholino[37] abolishes DlA immunoreactivity but fails to elicit polarity defects in a wild-type background (Supplementary Fig. S2c,d). In contrast, polarity defects are observed upon dla knock-down in *dld*^{ar33} mutants (Fig. 2c,d).

Notch receptor activation results in the γ-Secretase-mediated release of NICD into the cytoplasm, allowing NICD nuclear entry and transcriptional activation of target genes[1,4]. Blocking Notch signaling using two different

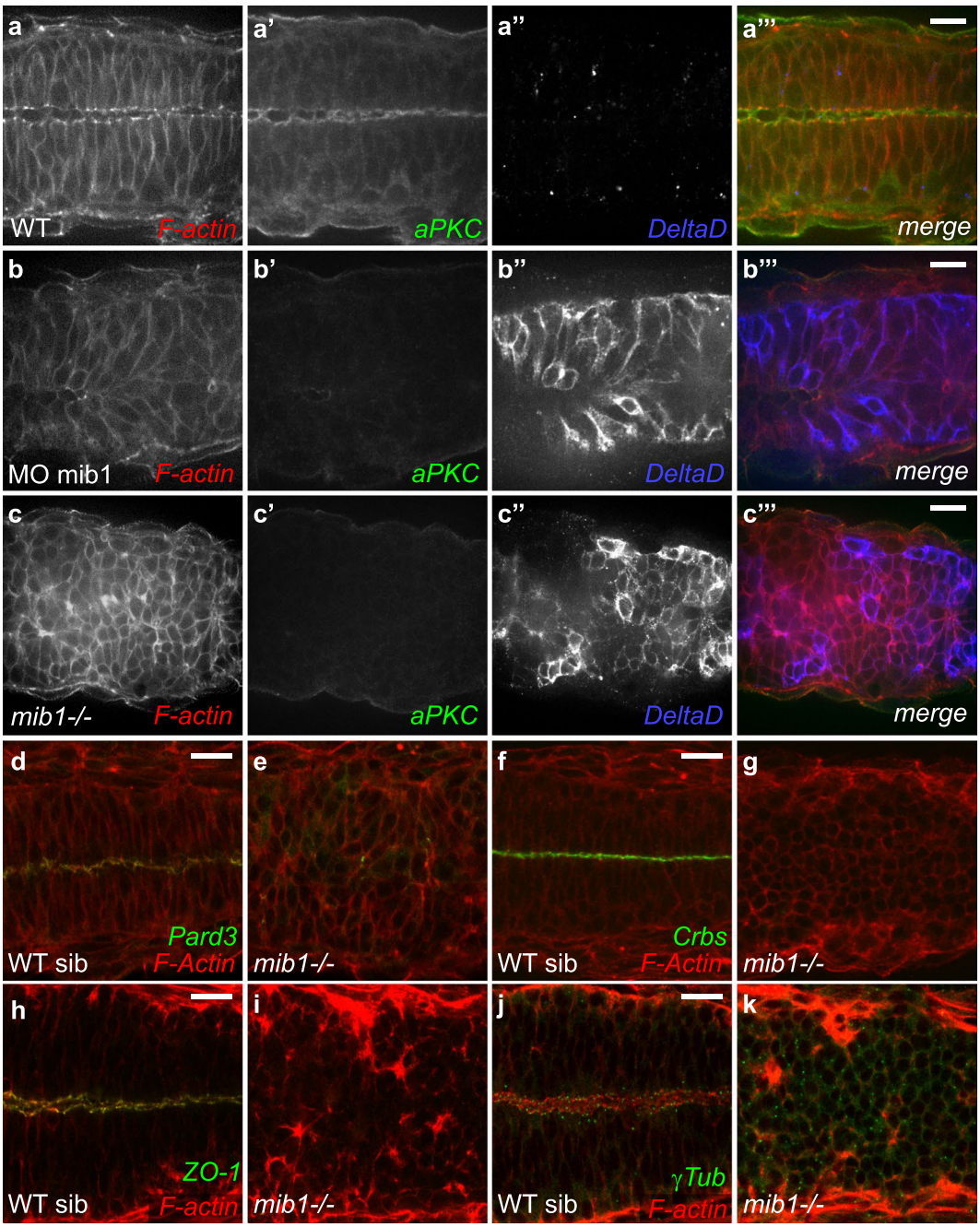

Figure 1. Mindbomb1 is required for zebrafish spinal cord morphogenesis. (**a**,**b**) Morpholino knock-down of mib1 disrupts apical aPKC enrichment and neuro-epithelial morphology (outlined by F-actin staining) in 15/19 embryos. (**c**) A similar disruption of apico-basal polarity is observed in *mib1* mutants (n = 14). (**d**,**e**) *mib1* mutants fail to establish polarized Pard3 localization (**e**, n = 12). (**f**,**g**) No polarized Crumbs enrichment is observed in *mib1* mutants (**g**, n = 17). (**h**,**i**) The apical localization of the tight junction component ZO-1 is disrupted in *mib1* mutants (**i**, n = 16). (**j**,**k**) Centrosomes fail to move towards the neural tube midline in *mib1* mutants (**k**, n = 16). (**a**–**c**,**f**,**g**) 30 somites stage. **d**,**e**, 18 somites stage, (**h**–**k**) 22 somites stage. All images are dorsal views of the anterior spinal cord, anterior left. Scalebars: 20 µm.

pharmacological γ-Secretase inhibitors, DAPT[38] and LY411575[39], impaired the apico-basal polarization of the neural tube (Fig. 2e–h).

If the polarity phenotype of Mib1-depleted embryos is a consequence of the loss of Notch signaling, restoring Notch activity should rescue neuroepithelial morphogenesis. Accordingly RNA injection of NICD, which acts as a constitutively activated form of Notch[40], restores neural tube apico-basal polarity in *mib1*^{ta52b} mutant (Fig. 2i–l) or mib1 morphant (Supplementary Fig. S2e–h) embryos.

Upon nuclear entry NICD associates with RBPJ/Su(H)/CBF transcription factors to trigger target gene activation[1,4]. Misexpression of a dominant-negative Su(H) variant[41] impaired neuroepithelial morphogenesis and

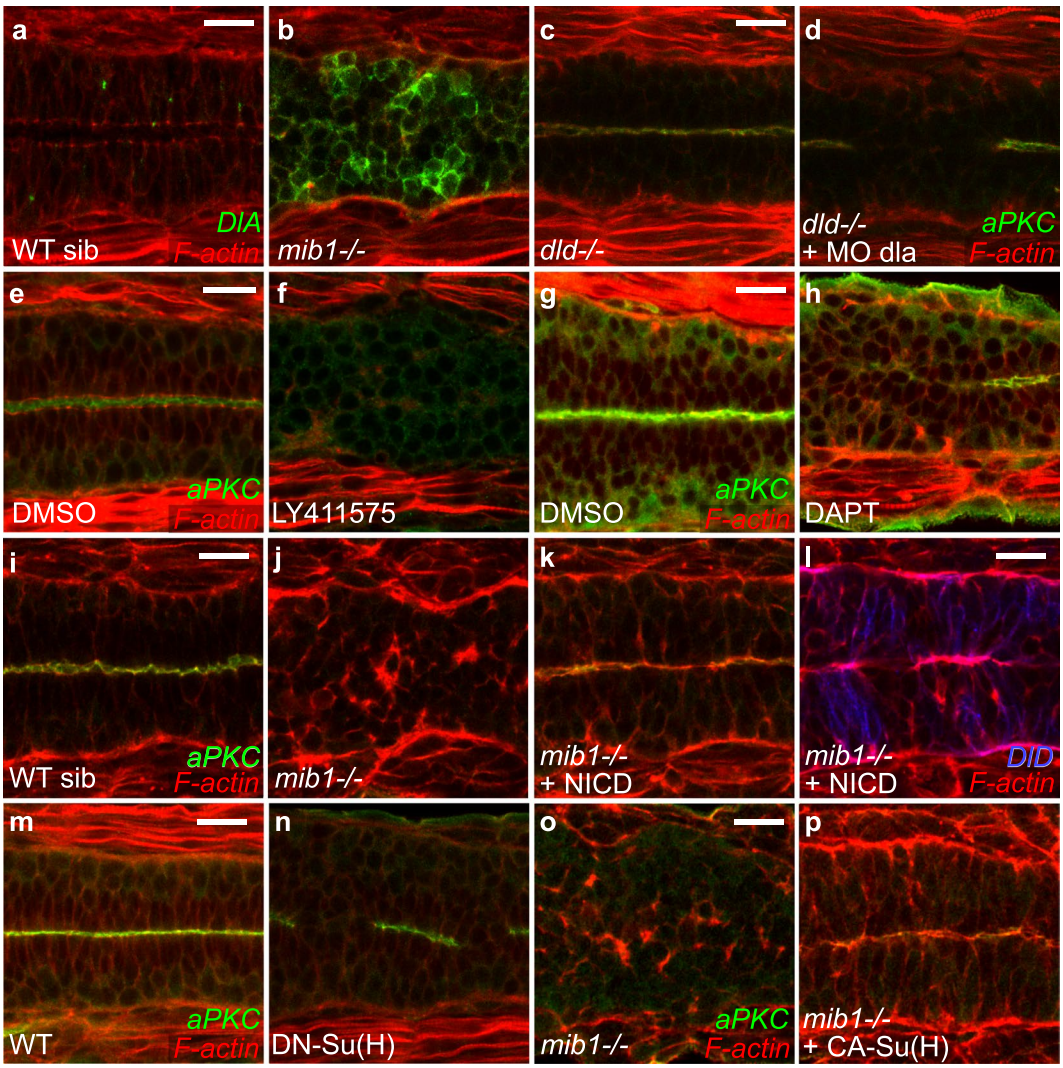

Figure 2. Notch pathway activity is required for spinal cord morphogenesis. (**a**,**b**) *mib1* loss of function prevents DlA internalization (n = 9). (**c**,**d**) Combined inactivation of *dld* and dla disrupts apico-basal polarity in 9/10 embryos. (**e**,**f**) The γ-Secretase inhibitor LY411575 disrupts apico-basal polarity (n = 18). (**g**,**h**) Similarly the γ-Secretase inhibitor DAPT perturbs polarity in 4/5 embryos. (**i**-**l**) RNA injection of a constitutively activated form of Notch (NICD) restores neuro-epithelial morphology and apical aPKC localisation (**k**) but not DeltaD endocytosis (**l**) in 22/22 *mib1* mutant embryos. (**m**,**n**) Polarity defects are observed in 20/46 embryos injected with RNA encoding dominant-negative Su(H) (DN-Su(H)). (**o**,**p**) RNA injection of constitutively activated Su(H) (CA-Su(H)) restores apico-basal polarity in 17/17 *mib1* mutants. All images are dorsal views of the anterior spinal cord, anterior left. (**a**–**f**) 22 somites stage, (**g**,**h**,**m**,**n**) 30 somites stage, (**i**–**l**,**o**,**p**) 16 somites stage. Scalebars: 20 µm.

polarized aPKC localization (Fig. 2m,n), consistent with the phenotype of CBF1 knock-out mice[42]. This result was confirmed through simultaneous morpholino knock-down of the two zebrafish Su(H)-homologues RBPJa&b (Supplementary Fig. S2i–l)[43]. Conversely, RNA microinjection of Constitutively Activated Su(H) (CA-Su(H)[41]) restores neuroepithelial tissue organization in *mib1*^{ta52b} mutants (Fig. 2o,p).

Therefore our observations show that not only Mib1 itself, but the activity of the entire canonical Notch pathway is required for zebrafish spinal cord morphogenesis.

Notch signaling is dispensable for the early establishment of floor plate apico-basal polarity. Previous studies have suggested that canonical Notch signaling is dispensable for the initial establishment, but required for the subsequent maintenance of neuroepithelial apico-basal polarity in fish and mice[42,44]. To address whether the defects of Mib1-depleted embryos similarly arise from a failure to maintain neuroepithelial polarity, we monitored the establishment of neural tube apico-basal polarity in wild-type sibling and *mib1*^{ta52b} mutant embryos.

The emergence of polarity has been studied mostly in the dorsal and medial regions of the zebrafish spinal cord[19,22]. In accordance with these studies, we find that the dorso-medial spinal cord does not show overt signs of

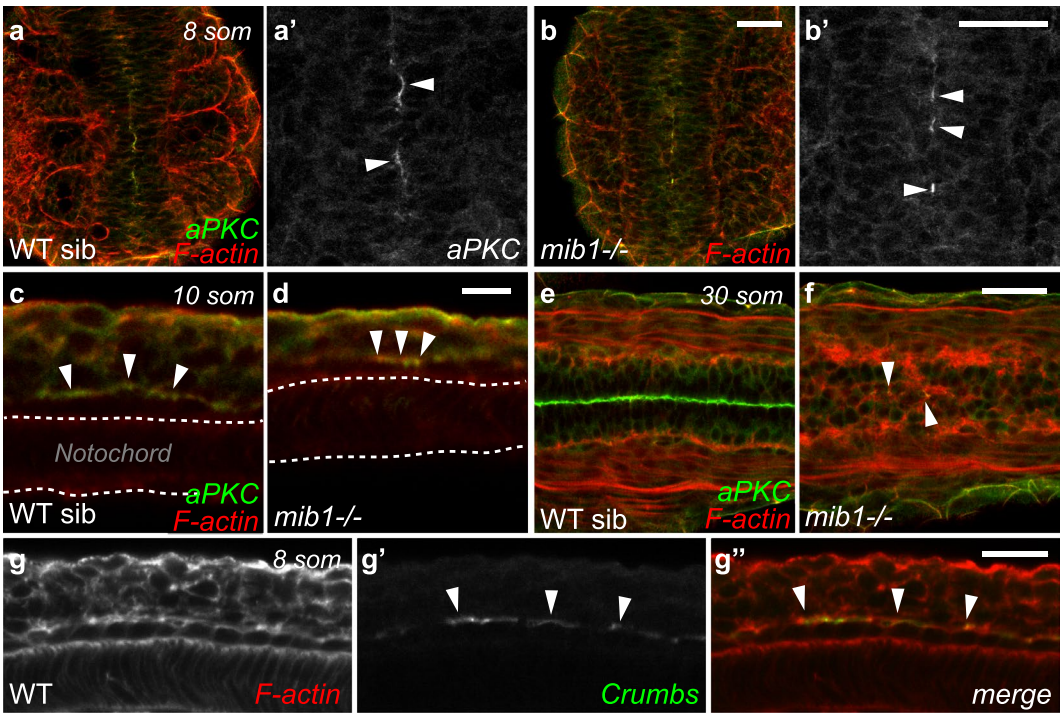

Figure 3. Notch signaling is dispensable for the emergence of floor plate apico-basal polarity. (**a**,**b**) At the 8 somites stage, similar discontinuous patches of polarized aPKC are detected in the ventral-most neural tube of WT siblings (**a**, n = 31) and *mib1* mutants (**b**, n = 14). Dorsal views, anterior up. (**a'**,**b'**) are high magnification views of the polarized aPKC signal. (**c**,**d**) aPKC is enriched at the apical surface of floor plate cells in 10 somites stage WT siblings (**c**, n = 8) and *mib1* mutants (**d**, n = 4). Lateral views, anterior left. (**e**,**f**) By the 30 somites stage polarized aPKC staining is reduced to few isolated cells in the ventral-most neural tube of *mib1* mutants (arrowheads in **f**, n = 5). Dorsal view, anterior left. (**g**) Crumbs protein accumulates at the apical surface of 8 somites stage floor plate cells (arrowheads). Lateral view, anterior left. Scalebars: (**a**,**b**) 40 µm, (**c**,**d**) 10 µm, (**e**–**g**) 20 µm.

apico-basal polarity prior to the 12 somites stage. However, we noticed that apico-basal polarity emerges much earlier in the ventral-most part of neural tube. From the 6 somites stage onwards, embryos display foci of polarized aPKC expression (Fig. 3a,c) that coalesce subsequently into a line (Fig. 3g', Supplementary Fig. S3). Lateral views of the neural tube show that this enrichment of aPKC (Fig. 3c) and Crumbs (Fig. 3g-g", Supplementary Fig. S3) corresponds to the apical surface of the cuboidal cells of the floor plate.

Notch signaling has been implicated in the differentiation of floor plate cells[45]. Mutations in *dla* or *mib1* have been reported to cause a severe reduction in the number of detectable floor plate cells by the end of the segmentation period[45]. Our observations confirm the occurrence of late floor plate defects (Fig. 3e,f), but also reveal that the initial establishment of floor plate cells and their apico-basal polarization do not require *mib1* function (Fig. 3a–d), and may therefore occur independently of Notch signaling. To test this hypothesis, we took advantage of the transgenic *tp1:bglob-GFP* Notch reporter line[46]. Until the 14 somites stage, i.e. mid-way through the embryonic segmentation period, reporter activity was absent from the floor plate, while adjacent tissues displayed fluorescence indicative of Notch signaling (Supplementary Fig. S3). This observation confirms that Notch signaling is dispensable for the initial formation and apico-basal polarization of the ventral-most cells of the neural tube.

Notch signaling restricts neurogenesis to allow the emergence of neuroepithelial tissue organization in the dorso-medial spinal cord. In contrast to the situation in the floor plate, Notch pathway activity is required for the morphogenesis of the more dorsal regions of the spinal cord (Fig. 4). To analyze the emergence of neuroepithelial tissue architecture and apico-basal polarity in the anterior spinal cord, we performed a time course analysis of polarized aPKC localization. In wild-type controls, aPKC becomes progressively enriched at the neural tube midline in the medial and dorsal aspects of the spinal cord from the 12 somites stage onwards (Fig. 4b,f,j,m,n), in accordance with the previously reported ventral to dorsal progression of neural tube maturation[19,47,48]. In contrast, *mib1*^{ta52b} mutants fail to display neuroepithelial tissue architecture and apico-basal polarity in the dorso-medial spinal cord at all stages examined (Fig. 4d,h,l,m,o). While previous studies have highlighted functions of Notch signaling in the late maintenance of neurectodermal apico-basal polarity[42,44], our findings show that zebrafish *mib1* is required already for the initial establishment of neuroepithelial tissue architecture.

Towards the end of neural development, most neural progenitors downregulate the expression of apical polarity proteins and differentiate into neurons[49]. As inactivation of *mib1* causes premature neuronal differentiation[6], we wondered whether the loss of neuroepithelial tissue organization in *mib1*^{ta52b} mutants might be correlated

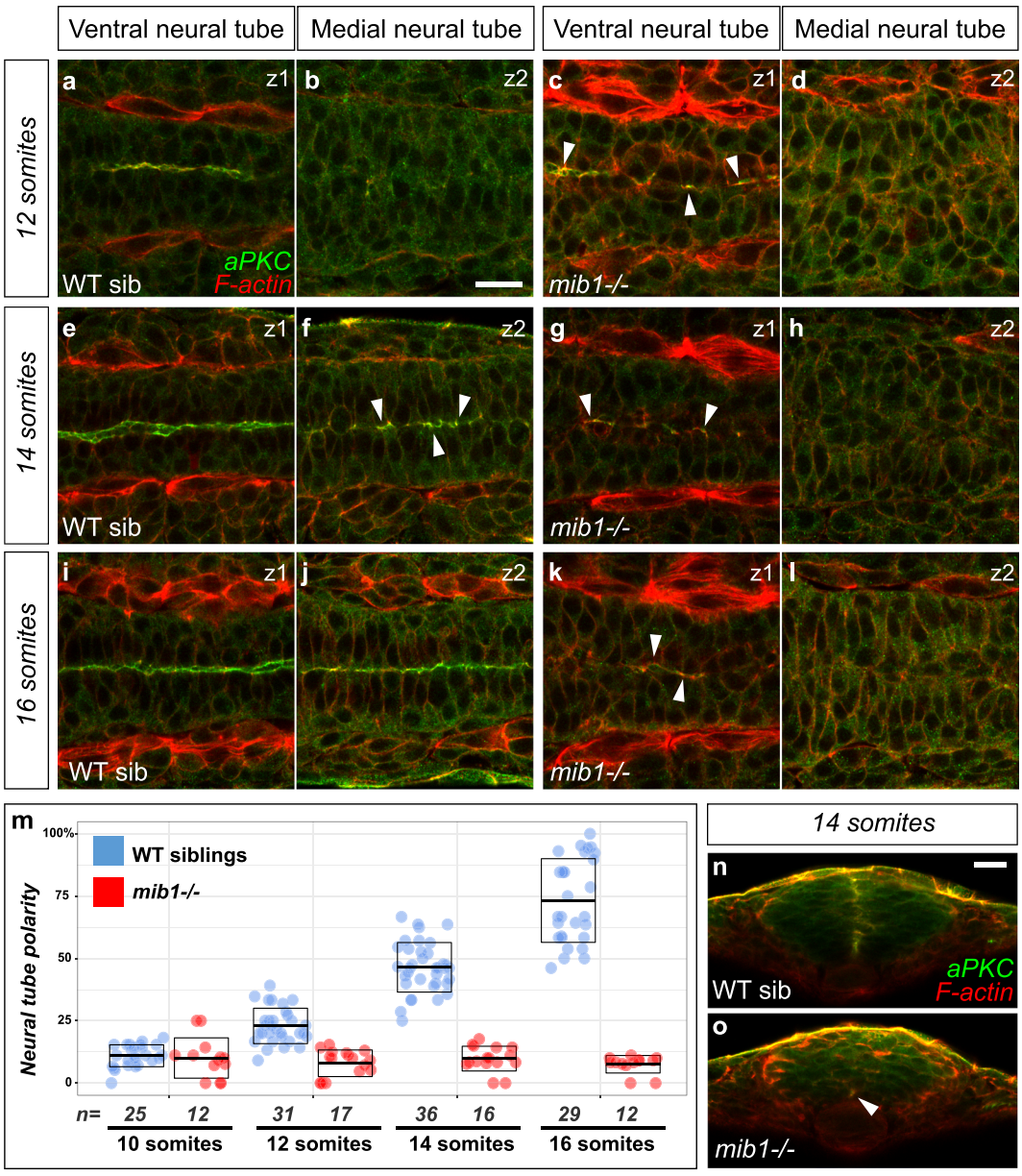

Figure 4. Notch signaling is required for the establishment of apico-basal polarity in the dorso-medial spinal cord. (**a**–**l**) Confocal sections taken at different dorso-ventral levels of the anterior spinal cord of WT sibling and *mib1* mutant embryos. Dorsal views, anterior left. z1 corresponds to the ventral-most extent of apico-basally polarized neuro-epithelial tissue (identified by aPKC staining), z2 is localized 12 µm more dorsally in the same embryo. Arrowheads indicate local foci of polarized aPKC in partially polarized tissue. (**a**–**d**) At the 12 somites stage polarized aPKC signal is detected in the ventral-most neural tube in WT sibling and *mib1* mutants. (**e**-**l**) At later stages polarity is progressively established in more dorsal regions of the neural tube in WT siblings (**f**,**j**), but remains limited to the ventral neural tube in *mib1* mutants (**g**,**h**,**k**,**l**). (**m**) Quantification of the progressive emergence of apico-basally polarity in the anterior spinal cord (see Methods). Boxes represent mean values ± SD. (**n**,**o**) Transversal sections (dorsal up) through the neural tube of 14 somites stage embryos. (**n**) Polarized aPKC staining starts to spread through the dorso-ventral extent of the neural tube in WT siblings. (**o**) In *mib1* mutants polarized aPKC enrichment remains limited to the ventral floor plate region (arrowhead). Scalebars: 20 µm.

with a failure to express genes governing neuroepithelial identity and apico-basal polarity. Zebrafish *sox19a* is expressed in undifferentiated neural precursors cells throughout the nervous system, similar to the expression of amniote *sox2*[50]. In accordance with a loss of neural precursors due to excessive neuronal differentiation, *mib1*^{ta52b} mutants display a premature loss of *sox19a* expression in the anterior spinal cord (arrow in Fig. 5d). Accordingly, all cells of the dorso-medial spinal cord start to express the marker of neuronal differentiation *elavl3* (Supplementary Fig. S4c).

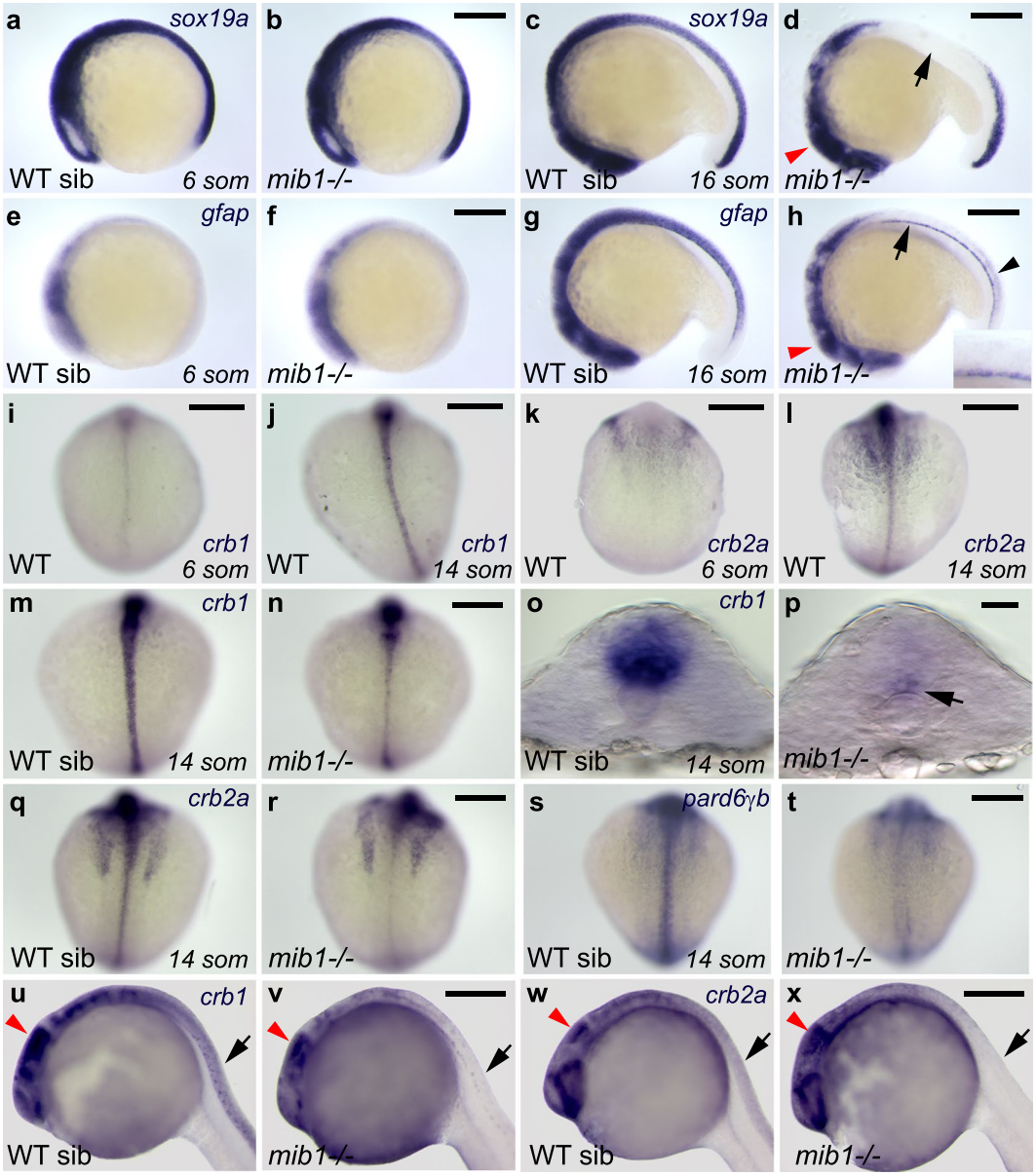

Figure 5. Notch signaling is required to allow the emergence of neuroepithelial identity. (**a**,**b**) The expression of the neuronal progenitor marker *sox19a* is similarly initiated in WT sibling (**a**) and *mib1* mutant embryos (**b**, n = 4). (**c**) By the 16 somites stage, *sox19a* expression is still present in the brain and anterior spinal cord of WT siblings. (**d**) In *mib1* mutants (n = 17) *sox19a* is lost in the anterior spinal cord (arrow) but partially retained in the brain (red arrowhead). (**e**,**f**) At the 6 somites stage, low levels of the radial glia marker *gfap* are detected in the brain region of WT siblings (**e**) or *mib1* mutants (**f**, n = 10). (**g**) By the 16 somites stage, WT siblings display *gfap* expression in the brain and spinal cord. (**h**) *mib1* mutants (n = 17) fail to upregulate *gfap* expression in the dorso-medial anterior spinal cord (inset). Reduced *gfap* expression levels are observed in the brain (red arrowhead) and caudal spinal cord (black arrowhead). Continuous *gfap* expression is retained in the floor plate (arrow). (**i**–**l**) The establishment of apico-basal polarity coincides with an upregulation of *crb1* (**i**,**j**) and *crb2a* (**k**,**l**) in the spinal cord. (**m**,**n**) Upregulation of *crb1* expression is impaired in *mib1* mutants (**n**, n = 11). (**o**,**p**) Residual *crb1* expression persists in the ventral-most spinal cord (arrow in **p**) of 14 somites stage *mib1* mutants. (**q**,**r**) *mib1* mutants display reduced *crb2a* expression in the spinal cord (**r**, n = 13). (**s**,**t**) *pard6γb* expression is lost in the neural tube of *mib1* mutants (**t**, n = 13). (**u**–**w**) In 30 somites stage *mib1* mutants *crb1* (**b**, n = 10) and *crb2a* (**d**, n = 10) expression are lost in the anterior spinal cord (black arrows) but partially retained in the brain (red arrowheads indicate the midbrain). (**a**–**h**, **u**–**x**) lateral views, anterior to the left, dorsal up. (**i**–**n**, **q**–**t**) dorsal views of the spinal cord, anterior up. (**o**,**p**) transversal sections of the neural tube, dorsal up. Scalebars: (**a**–**n**,**q**–**t**) 200 µm, (**o**,**p**) 20 µm, (**u**–**x**) 250 µm.

Radial glia cells are neural precursors that display apico-basal polarity and are crucial for the maintenance of neuroepithalial tissue architecture in the brain of zebrafish and higher vertebrates[10,11]. One of the hallmarks of radial glia is the expression of *glial fibrillary acidic protein* (*gfap*)[12,13]. In accordance with a lack of apico-basally

polarized neural precursor cells, *gfap* expression levels are very low in the presumptive spinal cord of 6 somites stage embryos (Fig. 5e). While wild-type sibling embryos upregulate *gfap* expression concomitantly with the establishment of apico-basal polarity (Fig. 5g), *mib1*^{ta52b} mutants fail to express *gfap* in the dorso-medial aspect of the anterior spinal cord (Fig. 5h).

Loss of Notch signaling impairs not only *gfap*, but also the expression of core components of the apico-basal polarity machinery belonging to the Par and Crumbs protein complexes[51]. While only low levels of *crumbs1* (*crb1) and crumbs2a (crb2a)* are detectable in the neural tube of wild-type 6 somites stage embryos (Fig. 5i,k), both genes display increased expression by the 14 somites stage (Fig. 5j,l). *mib1*^{ta52b} mutants fail to display this upregulation (Fig. 5m–r). Similarly, reduced expression levels of the Par complex component *pard6γb*[52] are observed in the spinal cord of *mib1*^{ta52b} mutants (Fig. 5s,t).

Region-specific control of neuroepithelial morphogenesis in the zebrafish spinal cord. Our observations uncover an essential role for the Notch-mediated suppression of neurogenesis in the regulation of neuroepithelial identity in the dorso-medial spinal cord. In addition, the analysis of neuroepithelial gene expressions confirms the existence of a different, Notch-independent regulation of apico-basal polarity in the ventral-most part of the neural tube. In this tissue, *crb1* transcripts are detectable already by the 6 somites stage (Fig. 5i), when first signs of polarized aPKC enrichment become detectable. While *mib1*^{ta52b} mutants fail to upregulate *crb1* expression in the dorso-medial neural tube where polarity is lost, *crb1* expression persists in the ventral-most cells where apico-basal polarity is retained (arrow in Fig. 5p). Similarly, *mib1*^{ta52b} mutant floor plate cells retain the expression of the neuroepithelial/radial glia marker *gfap* (arrow in Fig. 5h). Accordingly, the analysis of the neuronal differentiation marker *elavl3* reveals that, in contrast to more dorsal and lateral spinal cord derivatives, *mib1*^{ta52b} mutant floor plate cells do not undergo neuronal differentiation (Supplementary Fig. S4d).

In contrast to the spinal cord, *mib1*^{ta52b} mutant brains do still express *gfap* and the neuronal precursor marker *sox19a*, albeit at reduced levels (red arrowheads in Fig. 5d,h). Similarly, *crb1* and *crb2a* are still expressed in the brain but no more detectable in the dorso-medial spinal cord of 30 somites stage *mib1*^{ta52b} mutants (Fig. 5u–x).

The occurrence of *mib1*^{ta52b} mutant polarity phenotypes correlates with the differential regulation of neuroepithelial gene expression and neuronal differentiation. In the dorso-medial spinal cord of *mib1*^{ta52b} mutant embryos, all cells undergo neuronal differentiation (Fig. 6l', Supplementary Fig. S4c), polarity gene expression is lost (arrows in Fig. 5v,x), and so is apico-basal polarity (Fig. 6d,h,l). *mib1*^{ta52b} mutant hindbrains present only a partial neurogenic transformation (Fig. 6j') and a partial loss of neuroepithelial polarity (Fig. 6f,j). Finally, polarity gene expression is retained in *mib1*^{ta52b} mutant midbrains (red arrowheads in Fig. 5v,x). Accordingly, *mib1*^{ta52b} mutants display only a very minor increase in neurogenesis (Fig. 6j') and retain the neuroepithelial tissue architecture of the midbrain and MHB (Fig. 6b,j).

To determine whether the retention of apico-basal polarity in the MHB region of *mib1* mutants could be due to residual Notch signaling, we introduced the *tp1bGlob:GFP* reporter[46] into *mib1* mutants. Notch reporter activity is essentially undetectable at the MHB in both wild-type sibling and homozygous mutant animals (Fig. 6i",j"). These observations suggest that Notch signaling is largely dispensable for MHB development at the stages considered here.

Similar to *mib1* single mutants, *mib1; mib2* double mutant animals present a loss of apico-basal polarity at the level of the spinal cord, but retain neuroepithelial tissue organization in the MHB region (Supplementary Fig. S5, Supplementary Table S1). These findings show that Mindbomb protein function is not required for early MHB morphogenesis and extend previous studies suggesting that *mib2* is dispensable for early embryonic development[28].

Apico-basal polarity does not require Notch signaling between midline-crossing mitotic sister cells. A characteristic feature of the morphogenesis of the zebrafish neural tube is the occurrence of midline-crossing C-divisions. As Notch signaling between mitotic sister cells is important for cell fate assignment during later stages of zebrafish neurogenesis[11,53] we wondered whether Delta/Notch signaling between C-dividing sister cells might be important for apico-basal polarity?

To explore this possibility, *mib1*^{ta52b} mutant cells were transplanted into wild-type hosts. As Mib1 is essential for Delta ligand activity, no Delta/Notch signaling occurs between *mib1*^{ta52b} mutant mitotic sister cells. Despite this fact, mutant cells display a polarized localization of Pard3-GFP at the apical cell surface (Fig. 7a). Conversely, wild-type cells implanted into the dorso-medial spinal cord of *mib1*^{ta52b} mutants hosts fail to display polarized Pard3 localization (Fig. 7b). Spinal cord apico-basal polarity does therefore not require Delta/Notch signaling between midline-crossing mitotic sister cells.

Notch signaling provides a local permissive environment for neuroepithelial morphogenesis. In the mouse and zebrafish forebrain, cells undergoing neuronal differentiation present Delta ligands to activate Notch in neighboring cells and thereby maintain their radial glia identity[10,11,18]. If a similar mechanism is at work in the zebrafish spinal cord, Notch activity should be required cell autonomously to allow the emergence of neuroepithelial characteristics. To address this issue, we generated mosaic embryos in which Notch signaling is activated only in one half of the neural primordium (Fig. 7c–j, see Methods for details).

In a first set of experiments, RNAs encoding NICD and a red fluorescent membrane label (GAP43-RFP) were co-injected into one blastomere of two cell stage embryos. A second injection was performed to introduce green GAP43-GFP in the other blastomere (Fig. 7c,e). By the end of gastrulation embryos in which the progeny of the two injected blastomeres had populated the left and right sides of the animal were selected and grown further to analyze the morphology and behavior of cells in the neural primordium. In wild-type siblings, NICD-positive and

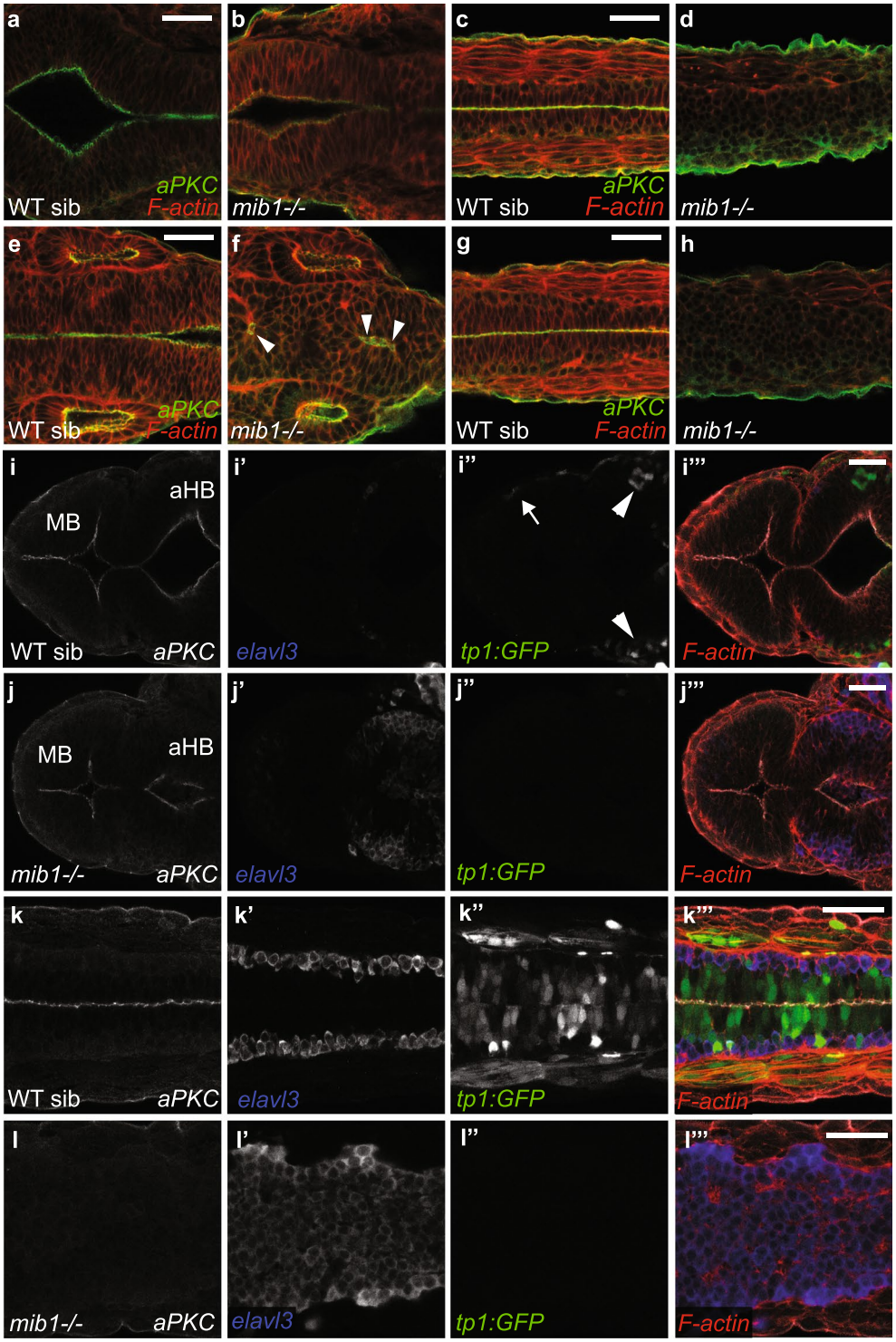

Figure 6. Notch loss of function differentially affects neuroepithelial polarity in the brain and spinal cord. (**a**–**h**) In *mib1* mutants neuroepithelial apico-basal polarity is maintained at the level of the midbrain-hindbrain boundary (**b**, n = 7), partially disrupted at the level of the hindbrain (**f**, arrowheads indicate residual polarized aPKC signal, n = 7) but completely lost in the dorso-medial spinal cord (**d**,**h**). (**g**,**h**) represent the most anterior and (**c**,**d**) the trunk spinal cord. (**i**–**l**) In WT siblings, the tp1bGlob:GFP (tp1:GFP) Notch reporter transgene indicates active signaling in a small number of cells in the anterior hindbrain (aHB, arrowheads in **i"**). More anteriorly, Notch activity is detected only in epidermal cells (arrow in **i"**) but not in the midbrain (MB) itself. *mib1* mutants present enhanced levels of neurogenesis (**j'**) and a partial disruption of apical aPKC localisation (**j**) at the level of the anterior hindbrain (n = 9). Only few elavl3-positive neurons are detected in the midbrain, which maintains neuroepithelial organization (**j**,**j'**). (**k**,**l**) At the level of the anterior spinal cord, WT sibling embryos display widespread Notch reporter activity (**k"**), basally localized elavl3-positive neurons (**k'**) and polarized aPKC enrichment at the apical neural tube midline (**k**, n = 6). *mib1* mutants present a loss of Notch

reporter expression (**l”**) and a lack of polarized aPKC localization (**l**, n = 8). Quantification of the area of the neural tube occupied by elavl3 positive cells reveals an increase in neurogenesis in *mib1* mutants (**l’**, 95.4 ± 2.6%) compared to WT siblings (**k’**, 31.7 ± 5.8%, p = 1.36E-07). Pictures (**a**,**c**), (**b**,**d**), (**e**,**g**), (**f**,**h**), (**i**,**k**) and (**j**,**l**) each represent the same embryo imaged at different antero-posterior locations. All images are dorsal views of 30 somites stage embryos, anterior left. Scalebars: 40 µm.

NICD-negative cells originating from the two neural tube halves both adopted an elongated morphology with cell bodies spanning the apico-basal extent of the neuroepithelium (Fig. 7d,d’).

A different result was observed when the same manipulation was carried out in *mib1*^{ta52b} mutants (Fig. 7e,f). In this case, only NICD-positive cells adopted a characteristic epithelial morphology, while NICD-negative cells failed to contact the neural tube midline and populated the basolateral aspect of the neural tube, a behavior suggestive of neuronal differentiation. To confirm that NICD enables the emergence of apico-basal polarity, we performed a second set of experiments where NICD was co-injected with Pard3-GFP (Fig. 7g–j). These experiments confirmed that NICD restores an apico-basal polarization of Pard3 in *mib*^{ta52b} mutant cells (Fig. 7j).

Our observations suggest that Notch signaling is required cell autonomously to allow the acquisition of neuroepithelial characteristics. However, these experiments also provide evidence that, even in conditions where Notch signaling is active only in one half of the cells of the neural primordium (Fig. 7e,i), *mib1*^{ta52b} mutant neural tubes can present a continuous apical neural tube midline, as indicated by cell morphology (Fig. 7f), Pard3-GFP accumulation (Fig. 7j) and aPKC localization (Fig. 7j”). While Notch signaling enables the emergence of neuroepithelial characteristics only in the cells where it is active, the presence of a fraction of Notch-activating cells is therefore sufficient to convey an overall neuroepithelial organization to the spinal cord.

Notch-mediated inhibition of neurogenesis is required for the morphogenetic movements of zebrafish spinal cord precursor cells. In wild type zebrafish, midline-crossing C-divisions cause the intermingling of cells originating from the two halves of the neural tube (Fig. 7d,d’)[19,22]. Our experiments in which Notch signaling was restored in one half of the *mib1*^{ta52b} mutant neural primordium suggested that only NICD-positive but not NICD-negative cells may be able to cross the neural tube midline (Fig. 7f-f”,j-j”). The midline-crossing of spinal cord cells has been proposed to confer a morphogenetic advantage for zebrafish spinal cord development[20,23,27], but the regulation of this behavior is poorly understood. In particular, it is not clear how this behavior is linked to neurogenic Notch signaling and neuronal differentiation. We decided to address this issue in *mib1*^{ta52b} mutants.

To visualize the midline-crossing of neural tube cells, one blastomere of two cell stage embryos was injected with GAP43-GFP RNA (Fig. 8a–j, Supplementary Fig. S6a–h). By the end of gastrulation, embryos in which the progeny of the injected blastomere occupied only the left or the right half of the embryo were selected for further analysis. Midline-crossing of neural tube cells is most prevalent from 14 to 18 hpf[19,22]. Accordingly, extensive crossing of GAP43-GFP positive cells to the contralateral side of the neural tube is observed by the 14 somites stage (i.e. 16 hpf) in wild-type siblings (Supplementary Fig. S6b,j). In contrast, midline crossing is reduced in *mib1*^{ta52b} mutants (Supplementary Fig. S6d,j). Additional experiments confirmed that midline crossing is still reduced at later developmental stages (Fig. 8d,k,l, Supplementary Fig. S6f,h,k, Supplementary Table S2), establishing that this phenotype is not simply due to developmental delay of mutant embryos.

NICD injection restored midline crossing in *mib1*^{ta52b} mutants (Fig. 8f,k, Supplementary Table S2), thereby establishing that this morphogenetic defect is due to a loss of Notch signaling and not to additional Notch-independent functions of Mib1 in the regulation of cell migration[35]. Accordingly, midline crossing is also reduced in *dld; dla* deficient embryos (Fig. 8j,m).

When Notch signaling activity is restored in *mib1*^{ta52b} mutant neural tubes through unilateral NICD injection, NICD-negative cells remain confined to one side of the neural tube and adopt a morphology and basolateral localization that is indicative of neuronal differentiation (Fig. 7f’). Staining with the neuronal differentiation marker elavl3 confirmed the neuronal identity of NICD-negative, non-crossing cells (Supplementary Fig. S7a,b). This observation raises the question whether the inability of *mib1*^{ta52b} mutant cells to cross the neural tube midline may be due to their premature neuronal differentiation? In accordance with this hypothesis, the midline-crossing of NICD-injected *mib1*^{ta52b} mutant cells correlates with a local inhibition of neuronal differentiation (Supplementary Fig. S7c–f).

While loss of Notch signaling and the resulting premature neuronal differentiation impair both the apico-basal polarization and the midline-crossing of neural tube cells, our experiments suggest that these two phenotypes are not strictly interdependent. Indeed, the injection of a dose of NICD that does not restore neural tube apico-basal polarity is already sufficient to rescue midline crossing (Fig. 8g,h,k, Supplementary Fig. S7k,l, Supplementary Tables S2 and S3).

The midline crossing of neural tube cells results in the intercalation of cells originating from the two sides of the neural tube, a behavior remindful of convergent extension movements[22,26]. We therefore wondered whether the shape of the spinal cord primordium is altered in *mib1*^{ta52b} mutants? In accordance with this hypothesis, transversal sections of the anterior spinal cord reveal an increased width-to-height ratio in *mib1*^{ta52b} mutants (Fig. 8n,o,q, Supplementary Table S4).

Loss of Notch signaling activity causes the premature loss of neuroepithelial progenitor cells in the anterior spinal cord (Fig. 5d). As a consequence of this depletion of dividing progenitor cells, *mib1*^{ta52b} mutants present a reduction in neural tube cell number (Supplementary Fig. S8a–d). This raises the question whether the observed alteration in *mib1*^{ta52b} mutant neural tube proportions may be a secondary consequence of this reduction in cell number? Our observations argue against this hypothesis: First, the injection of NICD promotes a partial

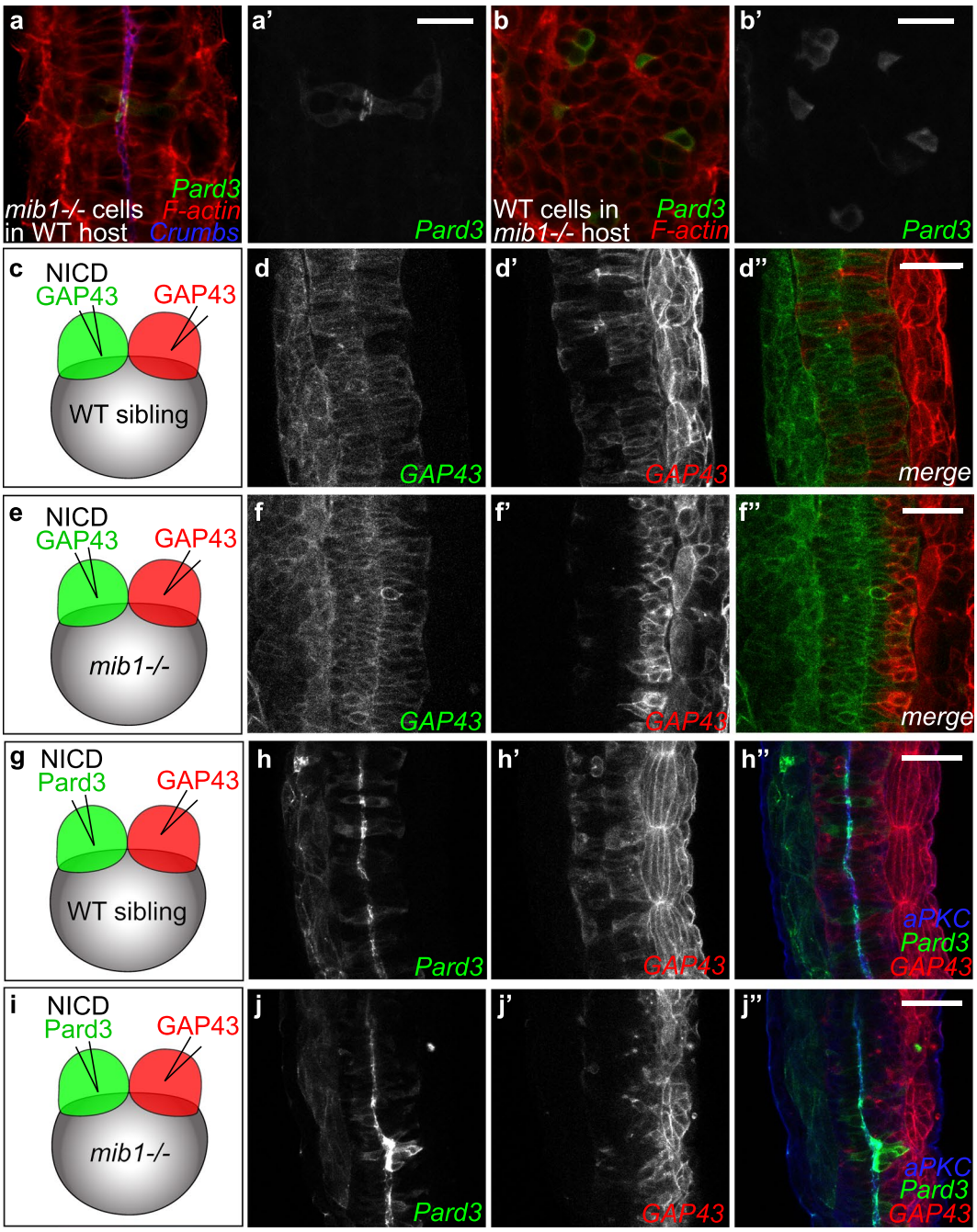

Figure 7. Dissection of the spatial requirement for Notch signaling in neural tube morphogenesis. (**a**,**a'**) Pard3-GFP expressing *mib1* mutant cells undergo correct polarization when transplanted into WT hosts (n = 30 cells in 6 embryos). (**b**,**b'**) In contrast, Pard3-GFP expressing WT cells fail to polarize when transplanted into *mib1* mutant hosts (n = 96 cells in 13 embryos). (**a**,**b**) are single confocal sections, (**a'**,**b'**) maximum projections of 5 slices separated by 2 µm intervals to visualize GFP-positive clones. (**c**-**f**) The two halves of the neural tube were labelled by injecting RNAs encoding red or green fluorescent membrane labels (GAP43) into the 2 blastomeres of 2-cell stage embryos (see Methods). (**c**,**d**) In WT sibling embryos half-injected with RNA encoding constitutively activated Notch (NICD), cells originating from both sides of the neural tube cross the neural tube midline to integrate the contra-lateral organ half (n = 7/7). (**e**,**f**) If NICD is half-injected into *mib1* mutants, NICD-containing cells display extensive midline crossing (**f**,**f"**), while the crossing of NICD-negative cells is reduced in 6/8 embryos (**f'**,**f"**). (**g**–**j**) One half of the embryo was injected with RNA encoding NICD Pard3-GFP, the other half with GAP43-RFP. (**g**,**h**) 6/6 WT sibling embryos display apical Pard3 accumulation (**h**) and bilateral midline crossing (**h**,**h'**). (**i**,**j**) In *mib1* mutants, NICD causes apico-basal polarization and midline crossing of Pard3-GFP positive cells in 6/6 embryos (**j**). NICD-negative GAP43-RFP positive cells fail however to cross the neural tube midline in 5/6 embryos (**j'**). Pictures represent dorsal views of the spinal cord (anterior up) at 30 somites (**a**,**b**), 18 somites (**d**,**f**) and 21 somites (**h**,**j**) stages. Scalebars: a,b 20 µm, (**d**,**f**,**h**,**j**) 40 µm.

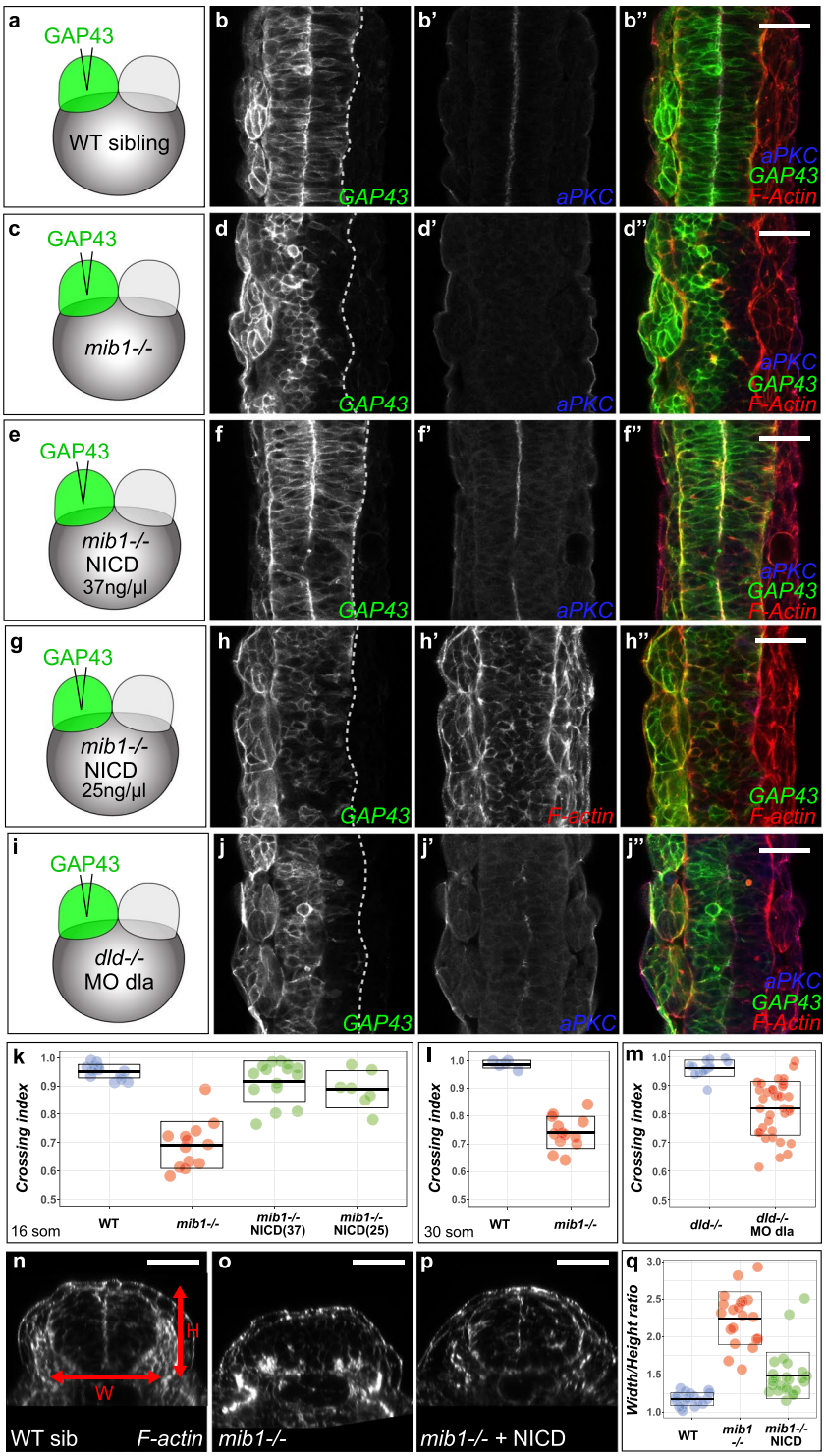

Figure 8. Notch loss of function impairs morphogenetic cell movements in the zebrafish spinal cord. (**a–i**) To label one half of the neural tube RNA encoding a fluorescent membrane label (GAP43-GFP) was injected into one blastomere of two cell stage embryos (see Methods). (**a**,**b**) In 16 somites stage WT siblings, cells from one half of the neural tube cross the organ midline to integrate the contra-lateral half. (**c**,**d**) In *mib1* mutants, neural tube cells fail to display this behavior. (**e**,**f**) RNA injection of constitutively activated Notch (NICD) at a concentration of 37.5 ng/µl restores apico-basal polarity (apical aPKC enrichment at the neural tube midline in **f'** compared to **d'**) and midline-crossing cell movements (**f**) in *mib1* mutants. (**g**,**h**) Injection of a lower dose of NICD (25 ng/µl) fails to restore neuroepithellial morphology (note the lack of apical F-actin accumulation at the neural tube midline in **h'**) but is sufficient to promote midline crossing (**h**). (**i**,**j**) Neural tube cells display reduced midline crossing in *dld*; *dla* compound mutant/morphants. (**k**) Quantification of neural tube midline crossing in WT, *mib1* mutants and NICD-injected *mib1* mutants (for details and statistical analysis see Methods, Supplementary Fig. S6i and Supplementary Table S2). (**l**) Reduced midline crossing is also observed

if WT sibling (crossing index 0.98 ± 0.01, n = 5) and *mib1* mutants (0.74 ± 0.06, n = 13) are compared at the 30 somites stage (p = 3.9E-10, see also Supplementary Fig. S6g,h). (**m**) Midline crossing is reduced in *dld; dla* mutants/morphants (0.82 ± 0.09, n = 36) compared to *dld* single mutants (0.96 ± 0.03, n = 14) (p = 2.1E-10). (**n**–**q**) Transversal sections of the anterior spinal cord used to measure neural tube width (W) and Height (H). *mib1* mutants (**o**) present an increased W/H ratio compared to WT siblings (**n**). NICD RNA injection restores neural tube proportions (**p**). (**q**) Quantification of W/H ratios, see Supplementary Table S4 for statistical analysis. (**b**,**d**,**f**,**h**,**j**) dorsal views of the anterior spinal cord at the 16 somites stage, anterior up. (**n**–**p**) transversal sections of the anterior spinal cord at 30 somites, after the completion of midline crossing. Scalebars: 40 µm. Boxes in (**k**,**l**,**m**,**q**) represent mean values ± SD.

but clearly significant (p = 1.14E-08) restoration of neural tube proportions (Fig. 8p,q) while triggering only a minor and non-significant (p = 0.129) increase in neural tube cell number (Supplementary Fig. S8a–d, see Supplementary Tables S4 and S5 for statistical analysis).

The effect of the loss of neuroepithelial progenitors on the number of neural tube cells is expected to become more pronounced as development proceeds. We performed therefore a second additional analysis of neural tube cell number and proportions at an earlier developmental time point. Despite having a number of neural tube cells similar to WT siblings (p = 0.23, Supplementary Fig. S8e,f,h), 24 somites stage *mib1*^{ta52b} mutants present already a significantly increased width-to-height ratio (p = 4.71E-06, Supplementary Fig. S8e–g), confirming thereby that the altered proportions of *mib1*^{ta52b} neural tubes are not a secondary consequence of changes in the number of cells that compose the neural primordium.

Taken together, our findings suggest that Notch-mediated suppression of neurogenesis is essential to allow neural tube cells to execute specific morphogenetic behaviors that direct the proper shaping of the spinal cord.

Discussion

The aim of the present study was to investigate how cell fate specification and morphogenesis are linked during the development of the zebrafish nervous system. In higher vertebrates, a dual relationship exists between the polarized epithelial organization of the neural plate and neurogenic Notch signaling. Notch activation promotes the maintenance of polarized radial glia cells[10] while the epithelial architecture of the neural primordium is itself required for Notch signaling[18]. In contrast, the early zebrafish neural plate does not display hallmarks of apico-basal polarity and the neural tube acquires a neuroepithelial tissue organization only several hours after the beginning of neurogenesis[19,20]. Our work shows that in spite of these differences, Notch signaling is required for zebrafish spinal cord morphogenesis.

Previous studies have implicated noncanonical, transcription-independent Notch signaling in the late maintenance of apico-basal polarity in the ventral neural tube[44]. In contrast, we show here that the E3-Ubiquitin ligase Mib1, a critical regulator of Delta internalization and Notch activation[6], is required to initiate the epithelialization of the neural primordium (Figs. 1 & 4), allowing thereby the formation of a neural tube whose tissue organization is similar to the one of tetrapods.

Beyond the control of Delta ligand endocytosis, Mib1 has been shown to inhibit Epb41l5, a protein that facilitates the disassembly of apical junctional complexes[34]. Likewise Neuralized, which promotes Delta internalization in *Drosophila*, exerts a Notch-independent activity in epithelial morphogenesis[54]. However, our observations show that in the zebrafish spinal cord not only Mib1 itself, but the complete canonical Notch pathway including its transcriptional mediators RBPJ/Su(H) are required for neuroepithelial morphogenesis (Fig. 2).

Already before the onset of neurogenesis, the neural plate of higher vertebrates displays hallmarks of epithelial organization[13]. Our findings show that in zebrafish, the primordium of the developing spinal cord does initially not express markers of polarized neural precursor cells (*gfap*) and components of the apico-basal polarity machinery (*crb1*, *crb2a*, *pard6γB*) (Fig. 5). In this context, Notch signaling is required to restrain neuronal differentiation and allow thereby the upregulation of the neuroepithelial gene expression program. Accordingly, Notch signaling deficient animals fail to display the progressive epithelialization observed in the neural tube of wild-type controls (Fig. 4).

Various mechanisms have been shown to govern the establishment of apico-basal polarity in different systems[51]. Notch inactivation in the dorso-medial spinal cord of the early zebrafish embryo causes excessive neuronal differentiation and the loss of neuroepithelial gene expression and apico-basal polarity (Fig. 5, Supplementary Fig. S4). It remains to be established whether Notch actively induces neuroepithelial properties or if, alternatively, these characteristics emerge by default as soon as Notch inhibits neuronal differentiation. As available tools do not allow manipulating Notch signaling and neurogenic differentiation independently of each other, it is currently not possible to address this question directly. Our experiments show that the establishment of apico-basal polarity in the floor plate (Fig. 3, Supplementary Fig. S3) and the MHB region (Fig. 6) do not require Mib1 function. In these developmental contexts, Notch signaling appears therefore not to be required to actively promote neuroepithelial tissue organization.

The differences in the mechanisms that control the morphogenesis of various parts of the nervous system are likely due to the fact that the importance of Notch signaling for developmental cell fate decisions varies according to the biological context. In contrast to more dorsal spinal cord cells, floor plate cells give rise essentially to glial derivatives[55]. Accordingly, *mib1* mutant floor plate cells do not undergo neuronal differentiation and retain their apico-basal polarity and expression of the radial glia marker *gfap*. At the level of the MHB, neurogenic differentiation is inhibited by the hairy-related transcription factor *her5*, which acts independently of Notch signaling[56]. This situation is different from the spinal cord where neurogenesis is regulated by the Notch-responsive *her4* gene[57].

Spinal cord development requires not only neurogenesis but also the execution of specific morphogenetic movements[20,21,23]. In the zebrafish, cells from one side of the neural tube invade the contra-lateral organ half by undergoing midline-crossing C-divisions[19,26,27]. We show that Notch-mediated suppression of neurogenesis is required to allow neural tube cells to execute their midline-crossing behavior (Fig. 8, Supplementary Figs S6 and S7).

Manipulations of PCP pathway activity have been shown to impair the midline-crossing behavior of neural tube cells[22,26]. Due to the general requirement of PCP signaling for embryonic convergent extension movements, these experiments have however not allowed to evaluate the actual impact of this morphogenetic behavior on the shaping of the neural tube. We show that in *mib1*^{ta52b} mutants, which do not display general convergent extension phenotypes, the cells of the neural primordium fail to display midline crossing and give rise to a misproportioned spinal cord (Fig. 8, Supplementary Fig. S8). Our findings suggest that through its ability to restrain neuronal differentiation, the Notch pathway provides a temporal window for neural tube cells to execute specific morphogenetic movements that determine the proportions of the spinal cord primordium prior to neuronal differentiation.

In conclusion, our findings show that, in addition to regulating the timing and identity of neuronal cell fate specification, Notch-mediated suppression of neurogenesis is essential to allow the acquisition of neuroepithelial tissue organization and the execution of specific morphogenetic movements that are required for the proper shaping of the zebrafish spinal cord.

Methods

Zebrafish strains and genotyping. Zebrafish strains were maintained under standard conditions and staged as previously described[58]. Zebrafish embryos were grown in 0.3x Danieau medium.

Depending on the experiment, *mib1* homozygous animals were identified using DeltaD immunostaining (mutant embryos can be identified by upregulated DlD signal at the cell membrane, Fig. 1c") or molecular genotyping (see below). From the 14 somites stage onwards, somitic segmentation defects allow a pre-selection of *mib1* homozygous mutant embryos prior to confirmation of the mutant genotype by one of the two above-mentioned approaches.

With the exception of the analysis of *mib1; mib2* double mutants (Supplementary Fig. S5) genetic inactivation of *mindbomb1* was performed using the *mib1*^{ta52b} allele[6]. A 4-primer-PCR was established to identify *mib1*^{ta52b} and WT alleles in a single PCR reaction. The following primers were used: 5′-ACAGTAACTAAGGAGGGC-3′ (generic forward primer), 5′-AGATCGGGCACTCGCTCA-3′ (specific reverse primer for the WT allele), 5′-TCAGCTGTGTGGAGACCGCAG-3′ (specific forward primer for the *mib1*^{ta52b} allele), and 5′-CTTCACCATGCTCTACAC-3′ (generic reverse primer). WT and *mib1*^{ta52b} mutant alleles respectively yield 303 bp and 402 bp amplification fragments. As some zebrafish strains present polymorphic *mib1* WT alleles, it is important to validate the applicability of this protocol before using it in a given genetic background.

Analysis of *mib1; mib2* double mutants was performed using the *mib1*^{tfi91} and *mib2*^{chi3} null mutant alleles[28]. The presence of the *mib1*^{tfi91} allele was detected using the primers 5′- ATGACCACCGGCAGGAATAACC-3′ (forward), and 5′- ACATCATAAGCCCCGGAGCAGCGC-3′ (reverse, 203 bp amplicon). The corresponding WT allele was detected using the primers: 5′- TAACGGCACCGCCGCCAATTAC-3′ (forward), 5′-GCGACCCCAGATTAATAAAGGG-3′ (reverse, 307 bp amplicon).

mib2^{chi3} mutant animals were identified by PCR amplification and sequencing of the mutation-carrying genomic region with the primers 5′-GCTCATCAGGGTCATGTAGAG-3′ (forward) and 5′-CTCCTATTGTTTGAGTGCAAAC-3′ (reverse, 254 bp amplicon).

PCR amplifications were carried out using GoTaq polymerase (Promega) at 1.5 mM MgCl2 using the following cycling parameters: 2 min 95 °C - 10 cycles [30 sec. 95 °C – 30 sec. 65 to 55 °C – 60 sec. 72 °C] – 25 cycles [30 sec. 95 °C – 30 sec. 55 °C – 60 sec. 72 °C] – 5 min 72 °C.

To inactivate *deltad* we used *dld/aei*^{AR33} [59] mutant embryos obtained through incrossing of homozygous mutant adult fish. To visualize Notch signaling activity, we used the *tp1bglob:eGFP* transgenic line[46].

mRNA and morpholino injections. Microinjections into dechorionated embryos were carried out using a pressure microinjector (Eppendorf FemtoJet). Capped mRNAs were synthesized using the SP6 mMessage mMachine kit (Ambion) and poly-adenylated using a polyA tailing kit (Ambion). RNA and morpholinos were injected together with 0.2% Phenol Red.

RNA microinjection was performed using the following constructs and concentrations: Mindbomb1-pCS2 + (125 ng/µl)[36]; Pard3-GFP-pCS2 + (50 ng/µl)[31]; DN-Su(H)-pCS2 + (600 ng/µl)[41]; CA-Su(H)-pCS2 + (40 ng/µl)[41]; Myc-Notch-Intra-pCS2 + (25–37.5 ng/µl)[40]; Gap43-GFP-pCS2 + (20 ng/µl) and GAP43-RFP-pCS2 + (30 ng/µl).

Morpholino oligonucleotides were injected at the indicated concentrations to knock down the following genes: mindbomb1: 5′-GCAGCCTCACCTGTAGGCGCACTGT-3′ (1000 µM)[6]; deltaA: 5′-CTTCTCTTTTCGCCGACTGATTCAT-3′ (250 µM)[37]; RBPJa: 5′-GCGCCATCTTCACCAACTCTCTCTA-3′ (50 µM) and RBPJb: 5′-GCGCCATCTTCCACAAACTCTCACC-3′ (50 µM). To ensure that the phenotypes of dla/*dld*^{AR33} morphant/mutants and RBPJa&b double morphants were not due to non-specific p53-mediated responses, we performed these experiments in the presence of a validated p53 Morpholino (5′-GCGCCATTGCTTTGCAAGAATTG-5′, 333 µM)[60].

Gamma-secretase inhibitor treatment. At mid-gastrulation zebrafish embryos were transferred to 0.3x Danieau medium containing 50 µM LY411575[39] (Sigma) or 100 µM DAPT[38] (Sigma) dissolved in DMSO. Embryos were raised till the 30 somites stage before being processed for antibody staining. Control embryos were mock-treated with DMSO alone.

Whole mount *in situ* hybridization. *In situ* hybridization was performed according to Thisse *et al.*[61]. DIG-labeled antisense RNA probes were transcribed from PCR products carrying the T7-promoter sequence (5′-TAATACGACTCACTATAGGG-3′) on the reverse primer. PCR amplicons for the different genes were flanked by the following sequences: *sox19a:* forward: 5′-CGATGTCGGGTGAAGATG-3′, reverse: 5′- CTGTCAAGGTTGTCAAGTCAC-3′ *gfap:* forward: 5′-TAAAGAGTCCACTACGGAGAGG-3′, reverse: 5′-GGCACCACAATGAAGTAATGTCC-3′, *crumbs1*: forward: 5′-TGTACCACCAGCCCATGTCATA-3′, reverse: 5′-cctcatcacagttttgacccac-3′; *crumbs2a:* forward: 5′-TGAGAGTGCCCCCTGCCTTAAT-3′, reverse: 5′-acagtcacagcggtagc-3′; *pard6γb:* forward: 5′-GACTACAGCAACTTTGGCACCAGCACTCT-3′, reverse: 5′-gtgatgactgtgccatcctcctc-3′.

Immunocytochemistry. Embryos were fixed in 4% paraformaldehyde in PEM (PIPES 80 mM, EGTA 5 mM, MgCl2 1 mM) for 1.5 hours at room temperature or overnight at 4 °C, before being permeabilized with 0.2% TritonX-100 in PEM-PFA for 30 minutes at room temperature. Subsequent washes and antibody incubations were performed in PEM + 0,2% TritonX-100. Primary antibodies used were: Mouse@DeltaD[6] (1:500, Abcam ab73331); Mouse@DeltaA[62] (1:250, ZIRC 18D2); Rabbit@aPKC[30] (1:250, Santa Cruz sc-216); Mouse@ZO1[63] (1:500, Invitrogen 1A12); Mouse@HuC/D[64] (1:500, Invitrogen 16A11); Rabbit@γ-Tubulin (1:250, Sigma T5192).

Cell transplantations. For cell transplantation embryos were maintained in 1x Danieau medium +5% penicillin-streptomycin. Donor embryos were labelled by injection of RNA encoding Pard3-GFP at the one-cell stage. Cell transplantations were carried out at late blastula/early gastrula stages. In each experiment, 20–30 cells were aspirated from the donor embryo using a manual microinjector (Sutter Instruments) and transplanted into the host embryo. Transplanted embryos were grown till the 30 somites stage in agarose-coated petri dishes with 0.3x Danieau and 5% penicillin-streptomycin before being fixed and processed for antibody staining.

Analysis of neural tube cell midline-crossing behaviour. To label one half of the neural tube, GAP43-GFP RNA was injected into one blastomere of 2-cell stage zebrafish embryos. The embryos were then grown till the bud stage, at which time point the localisation of the fluorescent cells was analysed using a fluorescence steromicroscope (Leica M205 FA). In a typical experiment, about 50% of the embryos displayed a unilateral localisation of GFP-positive cells and were kept to be grown till the desired stage before being fixed and processed for antibody staining. In contrast to the cells of the neural tube, somitic precursors do not cross the embryonic midline in the course of development. Consequently, successful half-injection results in a unilateral labelling of the somites that becomes visible at confocal analysis.

To quantify the extent of neural tube cell midline crossing, a crossing index was determined for each individual embryo as the fraction of the neural tube populated by GFP-positive cells (Supplementary Fig. S6i). Measurements were performed at the level of the medial neural tube. The total neural tube area and the GFP-positive area were outlined manually in Fiji using the F-actin and GFP channels.

To separately label the two opposite sides of the neural tube, 50 2-cell stage embryos were initially injected into one blastomere with RNA encoding the first fluorescent membrane label (e.g. GAP43-GFP). The presence of Phenol red in the injection mix allows identifying the injected blastomere for several minutes after injection. A second injection needle was then used to inject the second RNA (e.g. GAP43-RFP) into the other blastomere. Embryos were grown till the bud stage and screened for efficient double half injection as described above.

Microscopy and image analysis. For confocal imaging, embryos were mounted in 0.75% low melting point agarose (Sigma) in glass bottom dishes (MatTek corporation). Embryos were imaged on Spinning disk (Andor) or Laser scanning confocal microscopes (Zeiss LSM510, 710, 780 and 880) using 40x Water or 60x Oil immersion objectives. *In situ* gene expression patterns were documented on a Leica M205FA-Fluocombi stereomicroscope. Image analysis was performed using ImageJ (http://rbs.info.nih.gov/ij/) or Zeiss ZEN software.

For the quantification of the temporal progression of apico-basal polarity in the neural tube (Fig. 4m), we acquired confocal stacks spanning the entire dorso-ventral extent of the neural tube. The percentage of neural tube polarity was then calculated for each embryo as the number of confocal slices displaying polarized aPKC enrichment, divided by the total number of slices of the neural tube stack. Examples of individual confocal slices at different dorso-ventral locations are shown in Fig. 4a–l.

For the quantification of neurogenesis, we measured the fraction of the neural tube area that was positive for the neuronal marker elavl3 using Fiji. The total area of the neural tube was outlined manually using the F-actin signal. The area occupied by neuronal cells was estimated by applying a constant intensity threshold to the elavl3 channel.

For the analysis of cell number and width-to-height (W/H) ratio in the spinal cord, embryos were stained with fluorescent Phalloidin and DAPI and mounted in glass bottom dishes with the dorsal surface of the embryo facing the coverslip. Embryos were imaged using a Zeiss LSM880 confocal microscope. A line scan was performed at the border between the 2nd somite and the 3rd somite to obtain a transversal section of the spinal cord. Zeiss ZEN imaging software was used to measure the width and the height of the spinal cord.

The number of Dapi-positive nuclei by transversal neural tube section was quantified in Fiji using the manual multi-point selection tool. Due to the thickness of the neural tube, nuclei in the ventral part of the neural tube (i.e. farthest from the objective) appear dimmer than more dorsal ones. Contrast adjustments during the quantification procedure were therefore used to reliably quantify both dorsal and ventral nuclei.

Statistical analysis. Statistical analysis was carried out using the R/RStudio packages for statistical computing. Analysis of experiments involving more than two conditions was performed using Welch's Anova (oneway.test function), followed by a Games-Howell post-hoc test (posthocTGH function) for pairwise comparisons

between different experimental groups. For experiments involving only two experimental conditions, p-values were calculated using Welch's two-sample t-Test (t.test function). Mean values are indicated ± SD. Data normality and variance were analyzed using the stat.desc and leveneTest functions.

Use of research animals. Animal experiments were performed in the iBV Zebrafish facility (experimentation authorization #B-06-088-17) in accordance with the guidelines of the ethics committee Ciepal Azur and the iBV animal welfare committee.

Data Availability

The datasets generated and analysed during the current study are available from the corresponding author on reasonable request.

References

1. Hori, K., Sen, A. & Artavanis-Tsakonas, S. Notch signaling at a glance. *J Cell Sci* **126**, 2135–2140, https://doi.org/10.1242/jcs.127308 (2013).
2. Shin, J., Poling, J., Park, H. C. & Appel, B. Notch signaling regulates neural precursor allocation and binary neuronal fate decisions in zebrafish. *Development* **134**, 1911–1920 (2007).
3. Haddon, C. *et al*. Multiple delta genes and lateral inhibition in zebrafish primary neurogenesis. *Development* **125**, 359–370 (1998).
4. Bray, S. J. Notch signalling: a simple pathway becomes complex. *Nat Rev Mol Cell Biol* **7**, 678–689 (2006).
5. Chapouton, P. *et al*. Notch activity levels control the balance between quiescence and recruitment of adult neural stem cells. *J Neurosci* **30**, 7961–7974, https://doi.org/10.1523/JNEUROSCI.6170-09.2010 (2010).
6. Itoh, M. *et al*. Mind bomb is a ubiquitin ligase that is essential for efficient activation of Notch signaling by Delta. *Dev Cell* **4**, 67–82 (2003).
7. Le Borgne, R. & Schweisguth, F. Unequal segregation of Neuralized biases Notch activation during asymmetric cell division. *Dev Cell* **5**, 139–148 (2003).
8. Fürthauer, M. & González-Gaitán, M. Endocytic regulation of notch signalling during development. *Traffic* **10**, 792–802 (2009).
9. Gaiano, N., Nye, J. S. & Fishell, G. Radial glial identity is promoted by Notch1 signaling in the murine forebrain. *Neuron* **26**, 395–404 (2000).
10. Yoon, K. J. *et al*. Mind bomb 1-expressing intermediate progenitors generate notch signaling to maintain radial glial cells. *Neuron* **58**, 519–531, https://doi.org/10.1016/j.neuron.2008.03.018 (2008).
11. Dong, Z., Yang, N., Yeo, S. Y., Chitnis, A. & Guo, S. Intralineage directional Notch signaling regulates self-renewal and differentiation of asymmetrically dividing radial glia. *Neuron* **74**, 65–78, https://doi.org/10.1016/j.neuron.2012.01.031 (2012).
12. Kim, H. *et al*. Notch-regulated oligodendrocyte specification from radial glia in the spinal cord of zebrafish embryos. *Dev Dyn* **237**, 2081–2089, https://doi.org/10.1002/dvdy.21620 (2008).
13. Götz, M. & Huttner, W. B. The cell biology of neurogenesis. *Nat Rev Mol Cell Biol* **6**, 777–788, https://doi.org/10.1038/nrm1739 (2005).
14. Norden, C. Pseudostratified epithelia - cell biology, diversity and roles in organ formation at a glance. *J Cell Sci* **130**, 1859–1863, https://doi.org/10.1242/jcs.192997 (2017).
15. Miyamoto, Y., Sakane, F. & Hashimoto, K. N-cadherin-based adherens junction regulates the maintenance, proliferation, and differentiation of neural progenitor cells during development. *Cell Adh Migr* **9**, 183–192, https://doi.org/10.1080/19336918.2015.1005466 (2015).
16. McIntosh, R., Norris, J., Clarke, J. D. & Alexandre, P. Spatial distribution and characterization of non-apical progenitors in the zebrafish embryo central nervous system. *Open Biol* **7**, https://doi.org/10.1098/rsob.160312 (2017).
17. Kimura, Y., Satou, C. & Higashijima, S. V2a and V2b neurons are generated by the final divisions of pair-producing progenitors in the zebrafish spinal cord. *Development* **135**, 3001–3005 (2008).
18. Hatakeyama, J. *et al*. Cadherin-based adhesions in the apical endfoot are required for active Notch signaling to control neurogenesis in vertebrates. *Development* **141**, 1671–1682, https://doi.org/10.1242/dev.102988 (2014).
19. Geldmacher-Voss, B., Reugels, A. M., Pauls, S. & Campos-Ortega, J. A. A 90-degree rotation of the mitotic spindle changes the orientation of mitoses of zebrafish neuroepithelial cells. *Development* **130**, 3767–3780 (2003).
20. Araya, C., Ward, L. C., Girdler, G. C. & Miranda, M. Coordinating cell and tissue behavior during zebrafish neural tube morphogenesis. *Dev Dyn* **245**, 197–208, https://doi.org/10.1002/dvdy.24304 (2016).
21. Korzh, V. Stretching cell morphogenesis during late neurulation and mild neural tube defects. *Dev Growth Differ* **56**, 425–433, https://doi.org/10.1111/dgd.12143 (2014).
22. Tawk, M. *et al*. A mirror-symmetric cell division that orchestrates neuroepithelial morphogenesis. *Nature* **446**, 797–800 (2007).
23. Cearns, M. D., Escuin, S., Alexandre, P., Greene, N. D. & Copp, A. J. Microtubules, polarity and vertebrate neural tube morphogenesis. *J Anat* **229**, 63–74, https://doi.org/10.1111/joa.12468 (2016).
24. Hong, E. & Brewster, R. N-cadherin is required for the polarized cell behaviors that drive neurulation in the zebrafish. *Development* **133**, 3895–3905, https://doi.org/10.1242/dev.02560 (2006).
25. Alexandre, P., Reugels, A. M., Barker, D., Blanc, E. & Clarke, J. D. Neurons derive from the more apical daughter in asymmetric divisions in the zebrafish neural tube. *Nat Neurosci* **13**, 673–679 (2010).
26. Ciruna, B., Jenny, A., Lee, D., Mlodzik, M. & Schier, A. F. Planar cell polarity signalling couples cell division and morphogenesis during neurulation. *Nature* **439**, 220–224 (2006).
27. Buckley, C. E. *et al*. Mirror-symmetric microtubule assembly and cell interactions drive lumen formation in the zebrafish neural rod. *EMBO J* **32**, 30–44 (2013).
28. Mikami, S., Nakaura, M., Kawahara, A., Mizoguchi, T. & Itoh, M. Mindbomb 2 is dispensable for embryonic development and Notch signalling in zebrafish. *Biol Open* **4**, 1576–1582, https://doi.org/10.1242/bio.014225 (2015).
29. Matsuda, M. & Chitnis, A. B. Interaction with Notch determines endocytosis of specific Delta ligands in zebrafish neural tissue. *Development* **136**, 197–206 (2009).
30. Horne-Badovinac, S. *et al*. Positional cloning of heart and soul reveals multiple roles for PKC lambda in zebrafish organogenesis. *Curr Biol* **11**, 1492–1502 (2001).
31. von Trotha, J. W., Campos-Ortega, J. A. & Reugels, A. M. Apical localization of ASIP/PAR-3:EGFP in zebrafish neuroepithelial cells involves the oligomerization domain CR1, the PDZ domains, and the C-terminal portion of the protein. *Dev Dyn* **235**, 967–977, https://doi.org/10.1002/dvdy.20715 (2006).
32. Omori, Y. & Malicki, J. oko meduzy and related crumbs genes are determinants of apical cell features in the vertebrate embryo. *Curr Biol* **16**, 945–957, https://doi.org/10.1016/j.cub.2006.03.058 (2006).
33. Hong, E., Jayachandran, P. & Brewster, R. The polarity protein Pard3 is required for centrosome positioning during neurulation. *Dev Biol* **341**, 335–345, https://doi.org/10.1016/j.ydbio.2010.01.034 (2010).
34. Matsuda, M. *et al*. Epb41l5 competes with Delta as a substrate for Mib1 to coordinate specification and differentiation of neurons. *Development*. https://doi.org/10.1242/dev.138743 (2016).

35. Mizoguchi, T., Ikeda, S., Watanabe, S., Sugawara, M. & Itoh, M. Mib1 contributes to persistent directional cell migration by regulating the Ctnnd1-Rac1 pathway. *Proc Natl Acad Sci USA* **114**, E9280–E9289, https://doi.org/10.1073/pnas.1712560114 (2017).
36. Zhang, C., Li, Q. & Jiang, Y. J. Zebrafish Mib and Mib2 are mutual E3 ubiquitin ligases with common and specific delta substrates. *J Mol Biol* **366**, 1115–1128, https://doi.org/10.1016/j.jmb.2006.11.096 (2007).
37. Latimer, A. J., Dong, X., Markov, Y. & Appel, B. Delta-Notch signaling induces hypochord development in zebrafish. *Development* **129**, 2555–2563 (2002).
38. Geling, A., Steiner, H., Willem, M., Bally-Cuif, L. & Haass, C. A gamma-secretase inhibitor blocks Notch signaling *in vivo* and causes a severe neurogenic phenotype in zebrafish. *EMBO Rep* **3**, 688–694, https://doi.org/10.1093/embo-reports/kvf124 (2002).
39. Rothenaigner, I. *et al*. Clonal analysis by distinct viral vectors identifies bona fide neural stem cells in the adult zebrafish telencephalon and characterizes their division properties and fate. *Development* **138**, 1459–1469, https://doi.org/10.1242/dev.058156 (2011).
40. Takke, C. & Campos-Ortega, J. A. her1, a zebrafish pair-rule like gene, acts downstream of notch signalling to control somite development. *Development* **126**, 3005–3014 (1999).
41. Wettstein, D. A., Turner, D. L. & Kintner, C. The Xenopus homolog of Drosophila Suppressor of Hairless mediates Notch signaling during primary neurogenesis. *Development* **124**, 693–702 (1997).
42. Main, H., Radenkovic, J., Jin, S. B., Lendahl, U. & Andersson, E. R. Notch signaling maintains neural rosette polarity. *PLoS One* **8**, e62959 (2013).
43. Echeverri, K. & Oates, A. C. Coordination of symmetric cyclic gene expression during somitogenesis by Suppressor of Hairless involves regulation of retinoic acid catabolism. *Dev Biol* **301**, 388–403, https://doi.org/10.1016/j.ydbio.2006.10.003 (2007).
44. Ohata, S. *et al*. Dual roles of Notch in regulation of apically restricted mitosis and apicobasal polarity of neuroepithelial cells. *Neuron* **69**, 215–230 (2011).
45. Appel, B. *et al*. Delta-mediated specification of midline cell fates in zebrafish embryos. *Curr Biol* **9**, 247–256, doi:S0960-9822(99)80113-4 [pii] (1999).
46. Parsons, M. J. *et al*. Notch-responsive cells initiate the secondary transition in larval zebrafish pancreas. *Mech Dev* **126**, 898–912 (2009).
47. Zou, J., Wen, Y., Yang, X. & Wei, X. Spatial-temporal expressions of Crumbs and Nagie oko and their interdependence in zebrafish central nervous system during early development. *Int J Dev Neurosci* **31**, 770–782, https://doi.org/10.1016/j.ijdevneu.2013.09.005 (2013).
48. Yang, X., Zou, J., Hyde, D. R., Davidson, L. A. & Wei, X. Stepwise maturation of apicobasal polarity of the neuroepithelium is essential for vertebrate neurulation. *J Neurosci* **29**, 11426–11440, https://doi.org/10.1523/JNEUROSCI.1880-09.2009 (2009).
49. Hudish, L. I., Blasky, A. J. & Appel, B. miR-219 regulates neural precursor differentiation by direct inhibition of apical par polarity proteins. *Dev Cell* **27**, 387–398, https://doi.org/10.1016/j.devcel.2013.10.015 (2013).
50. Okuda, Y. *et al*. Comparative genomic and expression analysis of group B1 sox genes in zebrafish indicates their diversification during vertebrate evolution. *Dev Dyn* **235**, 811–825, https://doi.org/10.1002/dvdy.20678 (2006).
51. Rodriguez-Boulan, E. & Macara, I. G. Organization and execution of the epithelial polarity programme. *Nat Rev Mol Cell Biol* **15**, 225–242, https://doi.org/10.1038/nrm3775 (2014).
52. Munson, C. *et al*. Regulation of neurocoel morphogenesis by Pard6 gamma b. *Dev Biol* **324**, 41–54, https://doi.org/10.1016/j.ydbio.2008.08.033 (2008).
53. Kressmann, S., Campos, C., Castanon, I., Fürthauer, M. & González-Gaitán, M. Directional Notch trafficking in Sara endosomes during asymmetric cell division in the spinal cord. *Nat Cell Biol* **17**, 333–339, https://doi.org/10.1038/ncb3119 (2015).
54. Chanet, S. & Schweisguth, F. Regulation of epithelial polarity by the E3 ubiquitin ligase Neuralized and the Bearded inhibitors in Drosophila. *Nat Cell Biol* **14**, 467–476 (2012).
55. Bonilla, S. *et al*. Identification of midbrain floor plate radial glia-like cells as dopaminergic progenitors. *Glia* **56**, 809–820, https://doi.org/10.1002/glia.20654 (2008).
56. Geling, A., Plessy, C., Rastegar, S., Strähle, U. & Bally-Cuif, L. Her5 acts as a prepattern factor that blocks neurogenin1 and coe2 expression upstream of Notch to inhibit neurogenesis at the midbrain-hindbrain boundary. *Development* **131**, 1993–2006, https://doi.org/10.1242/dev.01093 (2004).
57. Takke, C., Dornseifer, P., v Weizsäcker, E. & Campos-Ortega, J. A. her4, a zebrafish homologue of the Drosophila neurogenic gene E(spl), is a target of NOTCH signalling. *Development* **126**, 1811–1821 (1999).
58. Kimmel, C. B., Ballard, W. W., Kimmel, S. R., Ullmann, B. & Schilling, T. F. Stages of embryonic development of the zebrafish. *Dev Dyn* **203**, 253–310, https://doi.org/10.1002/aja.1002030302 (1995).
59. Holley, S. A., Geisler, R. & Nüsslein-Volhard, C. Control of her1 expression during zebrafish somitogenesis by a delta-dependent oscillator and an independent wave-front activity. *Genes Dev* **14**, 1678–1690 (2000).
60. Robu, M. E. *et al*. p53 activation by knockdown technologies. *PLoS Genet* **3**, e78, https://doi.org/10.1371/journal.pgen.0030078 (2007).
61. Thisse, C. & Thisse, B. High-resolution *in situ* hybridization to whole-mount zebrafish embryos. *Nat Protoc* **3**, 59–69, https://doi.org/10.1038/nprot.2007.514 (2008).
62. Tallafuss, A., Trepman, A. & Eisen, J. S. DeltaA mRNA and protein distribution in the zebrafish nervous system. *Dev Dyn* **238**, 3226–3236, https://doi.org/10.1002/dvdy.22136 (2009).
63. Itoh, M., Nagafuchi, A., Yonemura, S., Kitani-Yasuda, T. & Tsukita, S. The 220-kD protein colocalizing with cadherins in non-epithelial cells is identical to ZO-1, a tight junction-associated protein in epithelial cells: cDNA cloning and immunoelectron microscopy. *J Cell Biol* **121**, 491–502 (1993).
64. Marusich, M. F. & Weston, J. A. Identification of early neurogenic cells in the neural crest lineage. *Dev Biol* **149**, 295–306 (1992).

Acknowledgements

This study was supported by a CNRS/INSERM ATIP/Avenir 2010 grant and an HFSP Career Development Award (00036/2010) to M.F. P.S. benefited from an FRM 4th year PhD fellowship (FDT20140930987). L.X. was supported by an ARC postdoctoral fellowship (PDF20121206203). V.M.S. is supported by the LABEX SIGNALIFE PhD program (ANR-11-LABX-0028-01). Confocal microscopy was performed with the help of the iBV PRISM imaging platform. *mib2*^{chi3} was obtained from the Japanese National Bioresource Project. We thank L. Bally-Cuif, Y.J. Jiang, M. Itoh, C. Kinter, J. Malicki, A. Oates, E. Ober, S. Sokol, and D. Stainier for the sharing of fish lines and reagents. We are grateful to S. Polès, M.A. Derieppe, R. Rebillard and F. Paput for excellent technical assistance.

Author Contributions

P.S. performed the experiments reported in Figures 1a-g, 2a–f,m,n, 4, 5i–x, 6a–h, 7a,b and S2a–h. V.M.S. performed the experiments of Figures 1h–k, 2i–l,o,p, 7c–j, 8, S2i–l, S5, S6, S7 and S8. L.X. performed the experiment displayed in Figure 2g,h. M.F. provided the data for Figures 3, 5a–h, 6i–l, S1, S3 and S4. M.F. designed and supervised the study and wrote the manuscript. All authors analyzed the data and contributed to the final version of the manuscript.

Additional Information

Supplementary information accompanies this paper at https://doi.org/10.1038/s41598-019-46067-1.

Competing Interests: The authors declare no competing interests.

Publisher's note: Springer Nature remains neutral with regard to jurisdictional claims in published maps and institutional affiliations.